Research Square

Preprints are preliminary reports that have not undergone peer review.
They should not be considered conclusive, used to inform clinical practice,
or referenced by the media as validated information.

Functional Screening and Biosafety Identify of the Potential Application of Let-7a in Injured Peripheral Nerve Regeneration

Qianqian Chen
Nanjing University
Qianyan Liu
Nantong University
Pan Wang
Nantong University
Tianmei Qian
Nantong University
Xinghui Wang
Nantong University
Sheng Yi
Nantong University
Shiying Li (lisy0379@ntu.edu.cn)
Nantong University https://orcid.org/0000-0001-5150-7299

Research Article

Keywords: let-7, Schwann cells, let-7a antagomir, chitosan, peripheral nerve regeneration

Posted Date: November 30th, 2021

DOI: https://doi.org/10.21203/rs.3.rs-1100490/v1

License: This work is licensed under a Creative Commons Attribution 4.0 International License.
Read Full License

Abstract

Proper supporting factor can possess the ability to enhance neuron regeneration, for instance, neurotrophic effects especially nerve growth factor (NGF). However, the *in vivo* applications of NGF are largely limited by its intrinsic disadvantages. Considering that let-7 targets and regulates NGF, and let-7 is also the core and harbor regulators in peripheral nerve repair and regeneration, we evaluated the potential application in clinical. We firstly screened the let-7a as the most ideal let-7 family molecular by gene expression analysis and functional approach. We further evaluated the *in vivo* safety, the cell permeability of 3 main cells in regeneration micro-environment, and the morphological and functional indicators. Our study provides an essential basis for *in vivo* application of let-7 and pictured a vision for the clinical translation of miRNA as a prospective alternative for regenerative medicine.

1 Introduction

Peripheral nerve injury is a common clinical problem that affects about 13 to 23 per 100,000 persons per year in the developed countries [1, 2]. Currently, the gold standard treatment for peripheral nerve injury is autologous nerve grafting. The application of autologous nerve graft, however, is largely limited by its intrinsic disadvantages such as limited donor nerve source, functional loss of donor nerve, and size differences of donor nerve and recipient nerve [3, 4]. Therefore, it has an urgent demand to develop and construct tissue engineered nerve grafts with better clinical effects to repair injured peripheral nerve.

Tissue engineered nerve grafts have been designed as a prospective alternative for regenerative medicine [5, 6]. Tissue engineered nerve grafts generally contain scaffolds and embedded supporting cells and/or biological cues. Morphological and cellular molecular studies demonstrated that immediately axonal regeneration involves the precise coordination of numerous cells in the environment to provide an optimal regeneration microenvironment. Macrophages, Fibroblasts, and Schwann cells gather to the injury site to perform different functions and help to establish an allowable regenerative pathway, as to achieve impaired peripheral nerve function recovery[7–9]. Many growth factors with neurotrophic effects, especially NGF benefit myelin sheath formation, possess the ability to enhance axon regeneration and have been used in neural tissue engineering [3, 10]. However, the *in vivo* applications of these growth factors are largely restricted by their low stability, short half-life periods, and high costs [11, 12]. Emerging studies showed that a variety of microRNAs (miRNAs) were dysregulated after peripheral nerve injury [3, 13–18]. Therefore, it is feasible to incorporate miRNAs into biomaterial scaffolds and to reshape the microenvironment so as to achieve injured nerve regeneration [10, 19–22].

Let-7, as the first identified human miRNA, is involved in many important biological processes [23–26]. The Let-7 family controls developmental timing and differentiation and strong evidence of let-7 has been shown to act as key regulators in various disease inflammation and cancer [27, 28]. Previous study showed that decreased let-7 elevated the secretion of NGF from Schwann cells, increased the proliferation and migration of Schwann cells *in vitro*, and promoted Schwann cell migration and axon outgrowth *in vivo* [29, 30]. The further study showed that let-7 is a core and harbor regulators affecting

nerve repair and regeneration [31]. Based on these hypotheses and preliminary study, we screened the ideal target member selection of the let-7 family, the cell permeability of 3 main cells in regeneration micro-environment, evaluated *in vivo* safety and indicated the morphological and functional to evaluate the repairing effect.

2 Materials And Methods

Ethics statement

Experimental animals were purchased from the Animal Experimental Center of Nantong University, Jiangsu, China. Experimental procedures were conducted in accordance with Institutional Animal Care guidelines of Nantong University and were ethically approved by Administration Committee of Experimental Animals, Jiangsu, China.

Schwann cell isolation, culture, and transfection

Primary Schwann cells were collected from sciatic nerve stumps of neonatal 1-day-old Sprague-Dawley (SD) rats, purified, and cultured as previous described [29]. Cultured Schwann cells were transfected with 20 nM let-7 mimic, 100 nM let-7 inhibitor, and corresponding mimic or inhibitor control (RiboBio, Guangzhou, Guangdong, China) using Lipofectamine RNAiMAX transfection reagent (Invitrogen, Carlsbad, CA, USA).

Quantitative RT-PCR

Total RNAs were isolated from cultured Schwann cells and reversely transcribed using TaqMan MicroRNA Reverse Transcription Kit (Applied Biosystems, Foster City, CA) and stem-loop RT primers (Ribobio). Quantitative RT-PCR was performed using QuantiNova SYBR Green PCR Kit (Qiagen, Hilden, Germany) on an Applied Biosystems Stepone real-time PCR System (Applied Biosystems, Foster City, CA). Relative expression levels of let-7 were determined by the ΔΔCt method.

EdU cell proliferation assay

Schwann cells were resuspended, seeded onto 96-well plates at a volume of 100 μL and a density of 2×10^5 cells/ml, and transfected with let-7 mimic, let-7 inhibitor, or the corresponding controls for 24 hours. 100 μM EdU was added to the cell culture medium and cells were cultured for additional 12 hours. After the fixation with 4% paraformaldehyde, the proliferation rate of Schwann cells was measured with Cell-Light EdU DNA Cell Proliferation Kit (RiboBio). Images were captured with a DMR fluorescence microscope (Leica Microsystems, Bensheim, Germany).

Transwell-based cell migration assay

Schwann cells transfected with let-7 mimic, let-7 inhibitor, or the corresponding controls were resuspended in DMEM medium and seeded onto the upper chamber of a 6.5 mm transwell with 8 μm

pores (Corning, Tewksbury, MA) at a volume of 100 μL and a density of 3×10^5 cells/ml. The bottom chamber of transwell was filled with 500 μL culture medium. After 24 hours incubation, Schwann cells left in the upper surface of the upper chamber were cleaned with a cotton swab while Schwann cells migrated to the bottom surface were stained with 0.1% crystal violet. Images were captured with a Leica DMI3000 B (Leica Microsystems). Migrated cells were dissolved in crystal violet with 33% acetic acid and measured the intensity of the absorbance of crystal violet staining using a SynergyTM 2 Multi-Mode Microplate Reader (BioTek, Burlington, VT, USA).

Biosafety assessment

Adult, male SD rats was anesthetized and injected with 100 nmol let-7a antagomir (RiboBio) dissolved in 1 ml saline through caudal vein injection. At 5 days after injection, rats were sacrificed and their hearts, livers, spleens, lungs, and kidneys were collected and fixed in 4% PFA. Hetamotylin-eosin staining was performed for histopathological examinations. At 5 days and 4 weeks after injection, rats were subjected to blood sample test. Blood cellular and electrolyte parameters, biochemical parameters, and immunological parameters were measured.

Flow cytometry analysis

Rats were subjected to sciatic nerve crush and 5 nmol let-7a antagomir was injected in each rat at the injury site immediately after nerve injury. Flow cytometry was conducted to measure the proportions of let-7a antagomir positive cells at 1 and 4 days after nerve injury. Rat sciatic nerve stumps were harvested, trypsinized, fixed, and incubated with primary antibodies rabbit anti-S100β antibody (1:100, Abcam, Cambridge, MA), rabbit anti-P4HB antibody (1:100, Abcam), mouse anti-CD68 antibody (1:200, Abcam). Cells were then stained with Alexa Fluor 488 donkey anti-rabbit IgG and subjected to flow cytometry analysis (BD Bioscience, San Jose, CA). The positive ratio of anti-let-7a containing cells was calculated with the following formula: Positive ratio=UR/(UR+LR) ×100%, where UR represented upper right and LR represented left right.

Animal surgery and application of let-7 antagomir

5 nmol let-7a antagomir was dissolved in 20 μL DEPC-treated water and mixed with 10 μL hydrogel (Beaver for Life Sciences, Suzhou, Jiangsu, China). The mixture of let-7a antagomir and hydrogel was injected into chitosan conduit to construct a let-7a antagomir. Adult, male SD rats (Anti-let-7a group) was subjected to 7 mm sciatic nerve transection and their nerve gaps were bridged with let-7a antagomir. Rats in the control group were bridged with chitosan scaffolds containing 5 nmol let-7a antagomir non-targeting control, 20 μL DEPC-treated water, and 10 μL hydrogel.

Immunohistochemistry and immunofluorescence staining

At 4 or 8 weeks after surgery, rat sciatic nerve tissues were mounted onto microscope slides, fixed in 4% PFA, and blocked with 5% goat serum. Sections were incubated with primary antibodies rabbit anti-S100β

antibody, rabbit anti-P4HB antibody, mouse anti-CD68 antibody, mouse anti-NF-200 (1:100; Sigma) and secondary antibodies goat anti-rabbit or anti-mouse 488 (1:500; Proteintech, Rosemont, IL) and cy3 (1:200, Proteintech) for axon morphological examination. Sections were stained with α-Bungarotoxin (1:500; Sigma) for motor endplate observation. Immunohistochemistrical images were taken under a fluorescence microscopy (Axio Imager M2, Carl Zeiss Microscopy GmbH, Jena, Germany).

Compound muscle action potential (CMAP) recording

At 8 weeks after surgery, rats in the control group and the Anti-let-7 group were used for CMAP recording by using a Keypoint 2 portable electromyography (Dantec, Denmark). Recording electrodes were inserted into the mid-belly of gastrocnemius and stimulating electrodes were inserted into the proximal and distal sciatic nerve stumps. An electric stimulus of 5 mV was delivered to evoke CMAP responses. CMAP amplitudes both at the proximal nerve stump and the distal nerve stumps were recorded.

CatWalk gait analysis

At 8 weeks after surgery, rats in the control group and the Anti-let-7a group were used for CatWalk gait analysis. The CatWalk XT system (Noldus Information Technology, the Netherlands) with a high-speed camera that detects digital images at a high-speed rate was used to determine the intensity of rat paws as previously described [32]. Sciatic function index (SFI) was calculated with the following formula: SFI=-38.3[(EPL-NPL)/NPL] +109.5[(ETS-NTS)/NTS] +13.3[(EIT-NIT)/NIT]-8.8, where EPL represented injured experimental site, NPL represented uninjured normal site, ETS represented toe spread, NTS represented the normal toe spread and NIT represented intermediate toe spread. A SFI value of -100 indicated loss of nerve function while a SFI value of 0 indicated normal nerve function.

Muscle weight measurement and Masson trichrome staining

At 4 and 8 weeks after surgery, the anterior tibial muscles and gastrocnemius muscles of rats in each group were collected to determine muscle wet weight ratio. Muscles on both the injured site and the contralateral uninjured site were weighed. The wet weight ratio was calculated by dividing the wet weight of muscle on the injured site to muscle on the contralateral uninjured site. The belly of anterior tibial muscle was collected, paraffin embedded, and stained with Masson trichrome. Muscle fibers were stained in red while collagen fibers were stained in blue.

Statistical analysis

Student’s t-test and ANOVA by Dunnett’s post hoc test were used to compare the statistical differences among groups. Statistical analysis and histograms were conducted with GraphPad Prism 6.0 (GraphPad Software, Inc., La Jolla, CA). A p-value < 0.05 was considered significant.

3 Results

let-7a, let-7c, and let-7d were highly expressed in Schwann cells, fibroblasts, and macrophages

The let-7 miRNA family contains many family members, including let-7a, let-7b, let-7c, let-7d, let-7e, let-7f, and let-7i. Quantitative outcomes showed that let-7a, let-7c, and let-7d were the top 3 highest expressed miRNAs in Schwann cells (Fig. 1a) and fibroblasts (Fig. 1b) while these 3 members of the let-7 family were also highly expressed in macrophages (Fig. 1c).

Let-7a, let-7c, and let-7d induced changes of gene expressions of other family members of let-7

Notably, members of the let-7 family and their negative regulator LIN28 possess a double-negative feedback loop. Changes of one member of the let-7 family may further affect other members of the let-7 family via the regulatory effect of LIN28. Considering the importance of Schwann cells in peripheral nerve repair and regeneration, Schwann cells were transfected with the mimics of top 3 highest expressed let-7 miRNAs, let-7a, let-7c, and let-7d. Besides the elevation of the abundance of let-7a, transfection with let-7a mimic elevated the expressions of all other members of let-7d, let-7e, and let-7f (Fig. 2a). Analogously, transfection with let-7c mimic and let-7d mimic increased the expressions of let-7e and let-7f (Fig. 2b). Transfection with let-7d, however, did not significantly affect the expressions of other family members of let-7 (Fig. 2c). Schwann cells were further transfected with inhibitors of let-7a, let-7c, or let-7d. The inhibitors of let-7a, let-7c, and let-7d, by contrast with the mimic, reduced the expressions of some members of the let-7 family (Fig. 2d, 2e & 2f). Consistently, the same results were observed in fibroblasts (Fig. 2g& 2i) and macrophages (Fig. 2h & 2j) transfected with let-7a mimic and let-7a inhibitor. These studies indicated that let-7a is the most ideal molecule for studying the let-7 family.

Our previous study demonstrated that let-7d could strongly inhibit Schwann cell proliferation and migration[29]. Here, the functional effects of let-7a and let-7c were also examined. EdU cell proliferation assay showed that similar as let-7d mimic, Schwann cells transfected with let-7a and let-7c mimic exhibited significantly reduced cell proliferation rate (Fig. 3a). On the contrast, cells transfected with let-7a inhibitor, let-7c inhibitor, or let-7d inhibitor exhibited elevated cell proliferation rates (Fig. 3b). Transwell-based cell migration assay showed that let-7a mimic, let-7c mimic and let-7d mimic induced an inhibitory effect on Schwann cell migration while let-7a inhibitor, let-7c inhibitor, and let-7d inhibitor induced a promoting effect on Schwann cell migration (Fig. 3c&3d). These observations suggested that let-7a was the most ideal molecule for studying the let-7 family and let-7a could strongly suppress the proliferation and migration of Schwann cells.

Let-7a did not induce morphological, biochemical, or immunological changes

The biosafety of let-7a antagomir was examined by directly introducing high dose (100 nmol) of let-7a antagomir into rats by caudal vein injection. Morphological characteristics of rat heart, liver, spleen, lung, and kidney were determined by hetamotylin-eosin staining at 5 days after let-7a antagomir injection. The external appearances and weights of these organs in rats injected with let-7a antagomir were similar with rats injected with saline only (Fig. 4a). Images from hetamotylin-eosin staining further demonstrated that the histopathological properties of these organs were not affected by let-7a antagomir injection (Fig. 4b).

The examination of rat blood samples collected at 5 days and 4 weeks after let-7a antagomir injection showed that blood cellular and electrolyte parameters, biochemical parameters, and immunological parameters of rats treated with let-7a antagomir were not significantly different from saline-treated control rats (Table 1).

Table 1

Blood sample examinations of rats injected with let-7a antagomir. Blood cellular and electrolyte parameters, biochemical parameters, and immunological parameters of rats at 5 days and 4 weeks after let-7a antagomir injection were determined.

Parameters	5 days		4 weeks	
	Con	Anti-let-7a	Con	Anti-let-7a
Blood cellular parameters				
White blood cell (10^9/L)	3.55±0.15	3.80±1.56	3.50±0.23	4.17±0.12
Red blood cell (10^{12}/L)	6.05±0.72	7.31±0.37	7.24±0.11	7.07±0.14
Platelet (10^{11}/L)	7.58±1.94	4.79±1.16	4.97±0.88	7.21±1.26
Hemoglobin (g/L)	125.3.0±15.25	145.3±5.68	140.7±1.20	141.7±3.53
Liver and kidney function levels and blood electrolyte parameters				
Total bilirubin (μmol/L)	9.33±0.88	9.00±0.58	11.67±0.33	10.67±0.67
Blood urea nitrogen (mmol/L)	6.50±0.63	6.83±0.69	6.27±0.27	7.17±0.39
Creatinine (μmol/L)	37.33±1.20	39.67±3.33	37.33±0.88	36.00±1.53
Creatine kinase (U/L)	558.7±67.22	638.7±213.50	608.7±106.10	480.3±3.53
Glucose (mmol/L)	9.20±0.40	8.8±0.35	11.40±0.74	11.73±0.32
Sodium (mmol/L)	147.7±0.88	146.3±1.45	145.0±1.16	146.0±0.58
Kalium (mmol/L)	6.93±0.23	6.00±0.06	6.63±0.18	6.27±0.09
Chlorine (mmol/L)	100.00±0.58	97.00±1.00	96.67±1.77	98.33±0.33
Immunological markers				
Immunoglobulin G (g/L)	0.80±0.07	0.77±0.00	0.67±0.06	0.80±0.03
Immunoglobulin M (g/L)	0.20±0.06	0.20±0.03	0.23±0.01	0.19±0.02
Complement C3 (g/L)	0.27±0.03	0.23±0.03	0.30±0.00	0.27±0.03
Complement C4 (g/L)	0.030±0.006	0.027±0.003	0.027±0.007	0.027±0.003

let-7a antagomir realized sustained promoting effect on peripheral nerve regeneration

Rat sciatic nerve crush injury was performed and rat sciatic nerve stumps were subjected to flow cytometry analysis to determine whether let-7a antagomir could enter into cells. At 1 day post injury, let-7a antagomir positive ratios in Schwann cells, fibroblast, and macrophages were about 33.7%, 61.5%, and 81.1%, respectively. At 4 days post injury, let-7a antagomir positive ratios in Schwann cells, fibroblast, and macrophages were about 54.6%, 31.7%, and 78.3%, respectively (Fig. 5a). Immunofluorescence outcomes directly showed that the antagomir of let-7a could enter into Schwann cells, fibroblasts, and macrophages (Fig. 5b). The fluorescent signal of Cy3 could be detected at 4 weeks after the nerve grafting, suggesting that the controlled release of let-7 antagomir was achieved (Fig. 5c).

The effect of let-7a antagomir on peripheral nerve regeneration was examined by NF-200 staining. Quantitative analysis showed that the fluorescence of NF-200 in the distal nerve stump in the Anti-let-7 group was much less than in the normal group but significantly higher than the control group (Fig. 6a). The morphology of motor endplates in gastronomies muscles observed at 8 weeks showed that the motor endplates in the Anti-let-7 group were also obviously larger than those in the control group (Fig. 6b).

Let-7a antagomir benefited the functional recovery of injured peripheral nerves

CMAP recording showed that at 8 weeks after injury, in normal rat nerves, the peak amplitudes at both the proximal site and the distal site were about 15 mV. In the control group, the detected peak amplitudes were obviously lower. Peak amplitudes in the Anti-let-7a group were much higher than those in the control group, reached about 8 mV (Fig. 7a). Automatic CatWalk track analysis detected the functional of injured peripheral nerves rats was increasing recovered. The measurement of the intensities of rat hindpaw showed that in Anti-let-7a-injected rats, the force and touch of the injured hindpaw were more closed to that of the uninjured hindpaw. At 8 weeks after injury, rats in the control group had a SFI of around -87 while rats in the Anti-let-7 group had a significantly higher SFI value of around -70, suggesting that the functional recovery of injured sciatic nerves was much better in the Anti-let-7 group (Fig. 7b).

The weight and morphology of the target muscles were also measured. At 4 weeks after surgery, there existed no difference in-between the wet weight ratios of anterior tibial muscle and gastrocnemius muscle in the control group and the Anti-let-7 group. However, at 8 weeks after surgery, the wet weight ratios of anterior tibial muscle and gastrocnemius muscle in the Anti-let-7 group were significantly higher than those in the control group (Fig. 8a). Observations from Masson trichrome staining showed that compared with muscles in the control group, muscle fibers were much larger and collagen fibers were relatively less in the Anti-let-7 group at 4 and 8 weeks after surgery (Fig. 8b).

4 Discussion

Therapeutics targeting miRNAs have been proved to be potential treatments for genetic disorders and regenerative medicine [33–35]. Since miRNAs regulate cell fate of neurons and glial cells, the potential therapeutic applications of miRNAs in neural tissue engineering have engrossed much attention [36].

Here, we constructed a let-7 antagomir-incorporated biomaterials to bridge peripheral nerve gaps in rats and largely contributes to the translational use of miRNAs.

Quantitative analysis of these let-7 family members in Schwann cells, the main cell type in sciatic nerve stumps, showed that let-7a, let-7c, and let-7d were expressed in relatively high levels while let-7a was the most abundant. Schwann cells were transfected with these highly expressed miRNAs to examine their regulatory effects on the expressions of other members of the let-7 family. Transfection with let-7a mimic, let-7a inhibitor, let-7c mimic and let-7c inhibitor significantly affected the abundances of other let-7 family members, indicating that let-7a and let-7c would elicit synergetic effects to enlarge their effectiveness. Moreover, let-7a mimic and inhibitor showed the most robust effects on Schwann cell proliferation and migration. Therefore, let-7a antagomir was used for generating neural tissue engineered graft.

The cellular uptake and *in vivo* stability of miRNAs are main barriers of the effective delivery of miRNAs [36]. We examined the presence of let-7a antagomir by immunohistochemistry staining and found that let-7a antagomir could enter into Schwann cells, fibroblasts, and macrophages. To achieve a stable and controlled release of let-7a antagomir, we innovatively dissolved let-7a antagomir in DEPC-treated water and mixed let-7a antagomir with hydrogel. By using hydrogel as the stabilizer and repository of let-7a antagomir, we found that let-7a antagomir could exist in the injured site for at least 4 weeks after nerve injury and repair. The mixture of let-7a antagomir and hydrogel was then injected into the chitosan conduit to effectively deliver let-7a antagomir into the injured site. Chitosan possesses favorable biocompatibility, biodegradability, and permeability. In our laboratory, chitosan-based artificial nerve grafts have been applied for peripheral nerve regeneration for a long period of time [37–39]. Therefore, we took the advantages of the properties of chitosan, used the chitosan tube as a nerve guidance conduit, and achieved the local delivery of let-7a antagomir. The joint use of hydrogel and chitosan conduit provided a helpful method for the long storage and controlled local release of miRNA agomir and/or antagomir.

The biological effect of let-7a antagomir was fully investigated by histological, morphological, and electrophysiological examinations. Immunohistochemistry staining, CMAP recording, CatWalk gait analysis, muscle weight measurement, and Masson trichrome staining demonstrated that let-7a antagomir could significantly promote axon elongation, increase electrophysiological response and sciatic function index, prevent muscle atrophy, and improve nerve innervation. Histopathological, biochemical, and immunological examinations also indicated that there existed no obvious adverse effects of let-7a antagomir. Our study incorporated let-7a into neural artificial nerve graft and successfully achieved controlled long-time release of let-7a antagomir and significantly promoted the growth of axons and the reinnervation of target muscles. The *in vivo* application of let-7a antagomir offers the possibility to bypass the disadvantages of the direct use of NGF and provides an essential basis for the clinical translation of miRNA-incorporated therapy in neural regeneration.

Declarations

Acknowledgments

The author sincerely apologizes to those whose work was not cited due to time and space constraints.

Funding

This work was supported by the Collegiate Natural Science Fund of Jiangsu Province [16KJA310005], Priority Academic Program Development of Jiangsu Higher Education Institutions [PAPD], the Natural Science Foundation of Jiangsu Province [BK20200976] and the National Natural Science Foundation of China [31970968].

Competing Interests

The authors declare that they have no conflict of interest that could have appeared to influence the work reported in this paper.

Author’s Contributions

Conceived and designed the experiments: Shiying Li. Experiment conductance and data analyses: Qianqian Chen, Qianyan Liu, Pan Wang, Tianmei Qian, Xinghui Wang and Shiying Li. Contributed reagents/materials/analysis tools: Qianqian Chen and Shiying Li. Wrote the manuscript: Qianqian Chen, Sheng Yi and Shiying Li. All authors read and approved the final manuscript.

Consent to participate

Not applicable.

Consent for publication Ethics approval

Not applicable.

Availability of data and materials

Data will be made available from the corresponding author on reasonable request.

References

1. Li R, Liu Z, Pan Y, Chen L, Zhang Z, Lu L (2014) Peripheral nerve injuries treatment: a systematic review. Cell Biochem Biophys 68(3):449–454. doi: 10.1007/s12013-013-9742-1
2. Lolis AM, Falsone S, Beric A (2018) Common peripheral nerve injuries in sport: diagnosis and management. Handb Clin Neurol 158:401–419. doi: 10.1016/B978-0-444-63954-7.00038-0
3. Gu X, Ding F, Yang Y, Liu J (2011) Construction of tissue engineered nerve grafts and their application in peripheral nerve regeneration. Prog Neurobiol 93(2):204–230. doi: 10.1016/j.pneurobio.2010.11.002
4. Luo L, He Y, Jin L, Zhang Y, Guastaldi FP, Albashari AA et al (2021) Application of bioactive hydrogels combined with dental pulp stem cells for the repair of large gap peripheral nerve injuries. Bioact Mater 6(3):638–654. doi: 10.1016/j.bioactmat.2020.08.028
5. Katiyar KS, Burrell JC, Laimo FA, Browne KD, Bianchi JR, Walters A et al (2021) Biomanufacturing of Axon-Based Tissue Engineered Nerve Grafts Using Porcine GalSafe Neurons. Tissue Eng Part A.. doi: 10.1089/ten.TEA.2020.0303
6. Coy R, Berg M, Phillips JB, Shipley RJ (2021) Modelling-informed cell-seeded nerve repair construct designs for treating peripheral nerve injuries. PLoS Comput Biol 17(7):e1009142. doi: 10.1371/journal.pcbi.1009142
7. Vargas ME, Barres BA (2007) Why is Wallerian degeneration in the CNS so slow? Annu Rev Neurosci 30:153–179. doi: 10.1146/annurev.neuro.30.051606.094354
8. Jessen KR, Mirsky R (2016) The repair Schwann cell and its function in regenerating nerves. J Physiol-London 594(13):3521–3531. doi: 10.1113/Jp270874
9. Gordon T (2016) Nerve regeneration in the peripheral and central nervous systems. J Physiol-London 594(13):3517–3520. doi: 10.1113/Jp270898
10. Gu XS, Ding F, Williams DF (2014) Neural tissue engineering options for peripheral nerve regeneration. Biomaterials 35(24):6143–6156. doi: 10.1016/j.biomaterials.2014.04.064
11. Chen JR, Yang L, Guo L, Duan XJ (2012) Sodium hyaluronate as a drug-release system for VEGF 165 improves graft revascularization in anterior cruciate ligament reconstruction in a rabbit model. Exp Ther Med 4(3):430–434. doi: 10.3892/etm.2012.629
12. Chen RR, Mooney DJ (2003) Polymeric growth factor delivery strategies for tissue engineering. Pharm Res-Dordr 20(8):1103–1112.. doi: Doi 10.1023/A:1025034925152
13. Li SY, Yu B, Wang SS, Gu Y, Yao DB, Wang YJ et al (2012) Identification and Functional Analysis of Novel Micro-RNAs in Rat Dorsal Root Ganglia After Sciatic Nerve Resection. J Neurosci Res 90(4):791–801. doi: 10.1002/jnr.22814
14. Yu B, Zhou SL, Qian TM, Wang YJ, Ding F, Gu XS (2011) Altered microRNA expression following sciatic nerve resection in dorsal root ganglia of rats. Acta Bioch Bioph Sin 43(11):909–915. doi: 10.1093/abbs/gmr083
15. Yu B, Zhou SL, Wang YJ, Ding GH, Ding F, Gu XS (2011) Profile of MicroRNAs following Rat Sciatic Nerve Injury by Deep Sequencing: Implication for Mechanisms of Nerve Regeneration. Plos One6(9). doi: ARTN e2461210.1371/journal.pone.0024612

16. Zhou SL, Yu B, Qian TM, Yao DB, Wang YJ, Ding F et al (2011) Early changes of microRNAs expression in the dorsal root ganglia following rat sciatic nerve transection. Neurosci Lett 494(2):89–93. doi: 10.1016/j.neulet.2011.02.064
17. Lopez-Leal R, Diaz-Viraque F, Catalan RJ, Saquel C, Enright A, Iraola G et al (2020) Schwann cell reprogramming into repair cells increases miRNA-21 expression in exosomes promoting axonal growth. J Cell Sci 133(12). doi: 10.1242/jcs.239004
18. Ji XM, Wang SS, Cai XD, Wang XH, Liu QY, Wang P et al (2019) Novel miRNA, miR-sc14, promotes Schwann cell proliferation and migration. Neural Regen Res 14(9):1651–1656. doi: 10.4103/1673-5374.255996
19. Krutzfeldt J, Rajewsky N, Braich R, Rajeev KG, Tuschl T, Manoharan M et al (2005) Silencing of microRNAs in vivo with 'antagomirs'. Nature 438(7068):685–689. doi: 10.1038/nature04303
20. Yu B, Zhou SL, Yi S, Gu XS (2015) The regulatory roles of non-coding RNAs in nerve injury and regeneration. Prog Neurobiol 134:122–139. doi: 10.1016/j.pneurobio.2015.09.006
21. Leng Q, Chen L, Lv Y (2020) RNA-based scaffolds for bone regeneration: application and mechanisms of mRNA, miRNA and siRNA. Theranostics 10(7):3190–3205. doi: 10.7150/thno.42640
22. Ou L, Lan Y, Feng Z, Feng L, Yang J, Liu Y et al (2019) Functionalization of SF/HAP Scaffold with GO-PEI-miRNA inhibitor Complexes to Enhance Bone Regeneration through Activating Transcription Factor 4. Theranostics 9(15):4525-41. doi: 10.7150/thno.34676
23. Roush S, Slack FJ (2008) The let-7 family of microRNAs. Trends Cell Biol 18(10):505–516. doi: 10.1016/j.tcb.2008.07.007
24. Shell S, Park SM, Radiabi AR, Schickel R, Kistner EO, Jewell DA et al (2007) Let-7 expression defines two differentiation stages of cancer. P Natl Acad Sci USA 104(27):11400–11405. doi: 10.1073/pnas.0704372104
25. Su JL, Chen PS, Johansson G, Kuo ML (2012) Function and regulation of let-7 family microRNAs. Microrna 1(1):34–39. doi: 10.2174/2211536611201010034
26. Yuan J, Nguyen CK, Liu XH, Kanellopoulou C, Muljo SA (2012) Lin28b Reprograms Adult Bone Marrow Hematopoietic Progenitors to Mediate Fetal-Like Lymphopoiesis. Science 335(6073):1195–1200. doi: 10.1126/science.1216557
27. Chirshev E, Oberg KC, Ioffe YJ, Unternaehrer JJ (2019) Let-7 as biomarker, prognostic indicator, and therapy for precision medicine in cancer. Clin Transl Med 8(1). doi: ARTN 2410.1186/s40169-019-0240-y
28. Tang J, Guo WC, Hu JF, Yu L (2019) Let-7 participates in the regulation of inflammatory response in spinal cord injury through PI3K/Akt signaling pathway. Eur Rev Med Pharmaco 23(16):6767–6773. doi: 10.26355/eurrev_201908_18714
29. Li SY, Wang XH, Gu Y, Chen C, Wang YX, Liu J et al (2015) Let-7 microRNAs Regenerate Peripheral Nerve Regeneration by Targeting Nerve Growth Factor (vol 23, pg 423, 2015). Mol Ther 23(4):790. doi: 10.1038/mt.2014.255

30. Zhang JC, Zhang YQ, Chen L, Rao ZT, Sun YQ (2020) Ulinastatin Promotes Regeneration of Peripheral Nerves After Sciatic Nerve Injury by Targeting let-7 microRNAs and Enhancing NGF Expression. Drug Des Dev Ther 14:2695–2705. doi: 10.2147/Dddt.S255158
31. Wang XH, Chen QQ, Yi S, Liu QY, Zhang RR, Wang P et al (2019) The microRNAs let-7 and miR-9 down-regulate the axon-guidance genes Ntn1 and Dcc during peripheral nerve regeneration (vol 294, pg 3489, 2019). J Biol Chem 294(17):6695. doi: 10.1074/jbc.AAC119.008724
32. Tian NX, Xu Y, Yang JY, Li L, Sun XH, Wang Y et al (2018) KChIP3 N-Terminal 31-50 Fragment Mediates Its Association with TRPV1 and Alleviates Inflammatory Hyperalgesia in Rats. J Neurosci 38(7):1756–1773. doi: 10.1523/Jneurosci.2242-17.2018
33. Beavers KR, Nelson CE, Duvall CL (2015) MiRNA inhibition in tissue engineering and regenerative medicine. Adv Drug Deliver Rev 88:123–137. doi: 10.1016/j.addr.2014.12.006
34. Chew SY (2015) MicroRNAs in tissue engineering & regenerative medicine Preface. Adv Drug Deliver Rev 88:1–2. doi: 10.1016/j.addr.2015.07.001
35. Gori M, Trombetta M, Santini D, Rainer A (2015) Tissue engineering and microRNAs: future perspectives in regenerative medicine. Expert Opin Biol Th 15(11):1601–1622. doi: 10.1517/14712598.2015.1071349
36. Nguyen LH, Diao HJ, Chew SY (2015) MicroRNAs and their potential therapeutic applications in neural tissue engineering. Adv Drug Deliver Rev 88:53–66. doi: 10.1016/j.addr.2015.05.007
37. Fan WM, Gu JH, Hu W, Deng AD, Ma YM, Liu J et al (2008) Repairing a 35-mm-long median nerve defect with a chitosan/PGA artificial nerve graft in the human: A case study. Microsurg 28(4):238–242. doi: 10.1002/micr.20488
38. Hu N, Wu H, Xue CB, Gong YP, Wu J, Xiao ZQ et al (2013) Long-term outcome of the repair of 50 mm long median nerve defects in rhesus monkeys with marrow mesenchymal stem cells-containing, chitosan-based tissue engineered nerve grafts. Biomaterials 34(1):100–111. doi: 10.1016/j.biomaterials.2012.09.020
39. Yang YM, Gu XS, Tan RX, Hu W, Hu W, Wang XD et al (2004) Fabrication and properties of a porous chitin/chitosan conduit for nerve regeneration. Biotechnol Lett 26(23):1793–1797.. doi: DOI 10.1007/s10529-004-4611-z

Figures

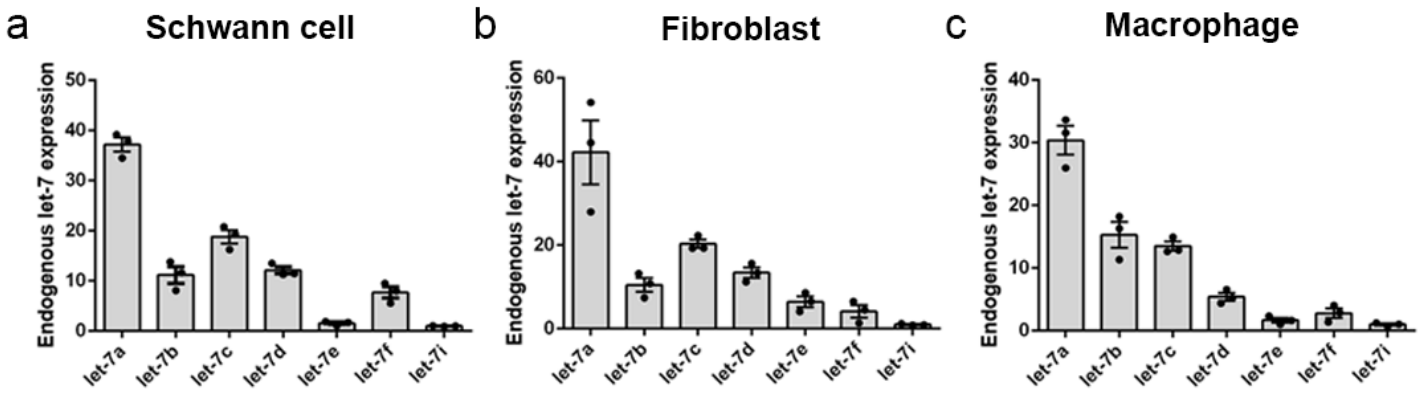

Figure 1

The expression levels of let-7 family members in (a) Schwann cells, (b) fibroblasts, and (c) macrophages. Histogram showed the relative expression levels of let-7a, let-7b, let-7c, let-7d, let-7e, let-7f, and let-7i.

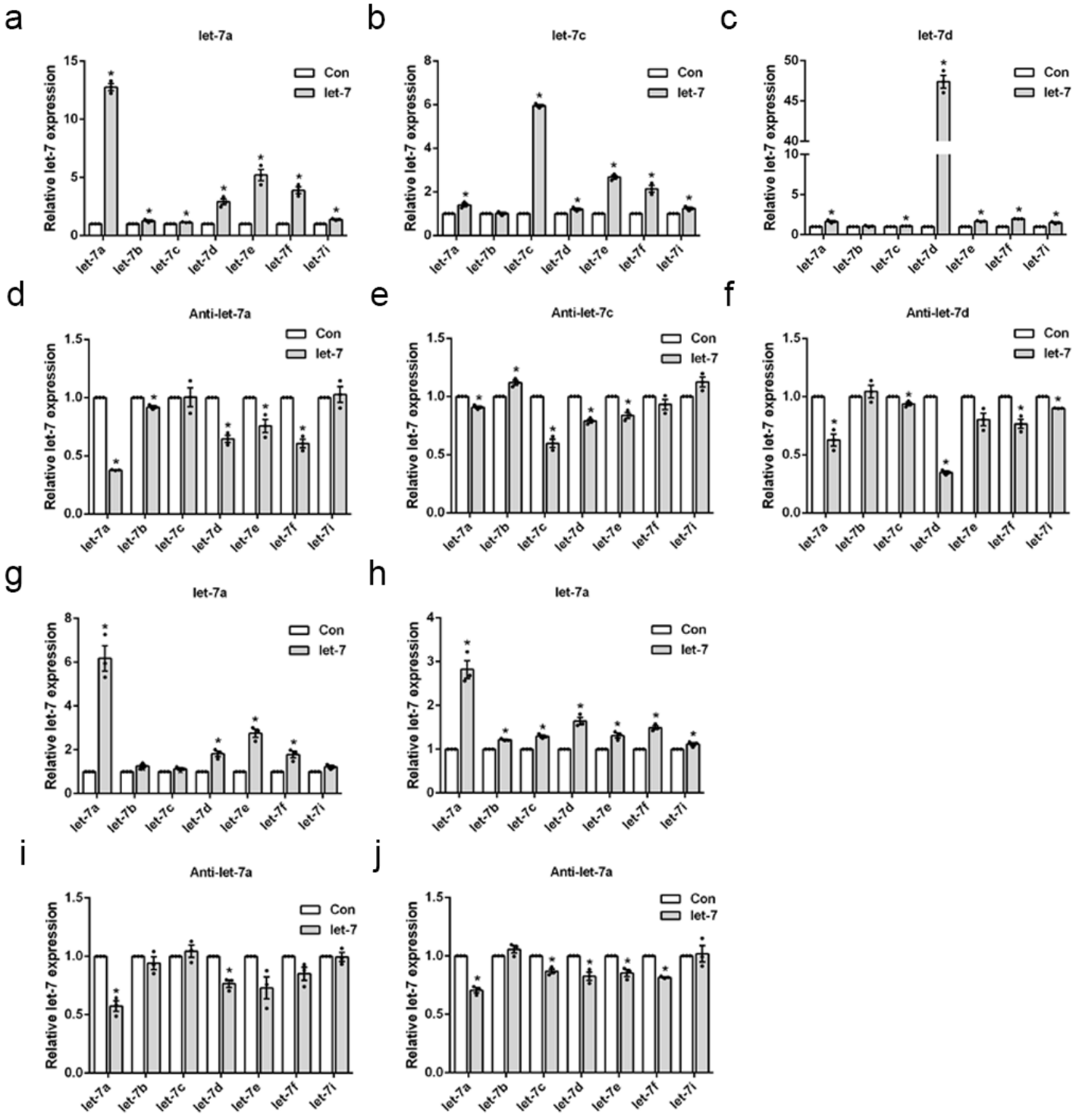

Figure 2

Effect of let-7a, let-7c, and let-7d on gene expression levels of other family members of let-7. Expression levels of let-7a, let-7b, let-7c, let-7d, let-7e, let-7f and let-7i after the transfection of (a) let-7a mimic, (b) let-7c mimic, (c) let-7d mimic, (d) let-7a inhibitor, (e) let-7c inhibitor, (f) let-7d inhibitor in Schwann cells. Expression levels of let-7a, let-7b, let-7c, let-7d, let-7e, let-7f and let-7i after the transfection of (a) let-7a mimic, (b) let-7a inhibitor in Fibroblasts; (c) let-7a mimic, (d) let-7d inhibitor in Macrophages. *p-value < 0.05.

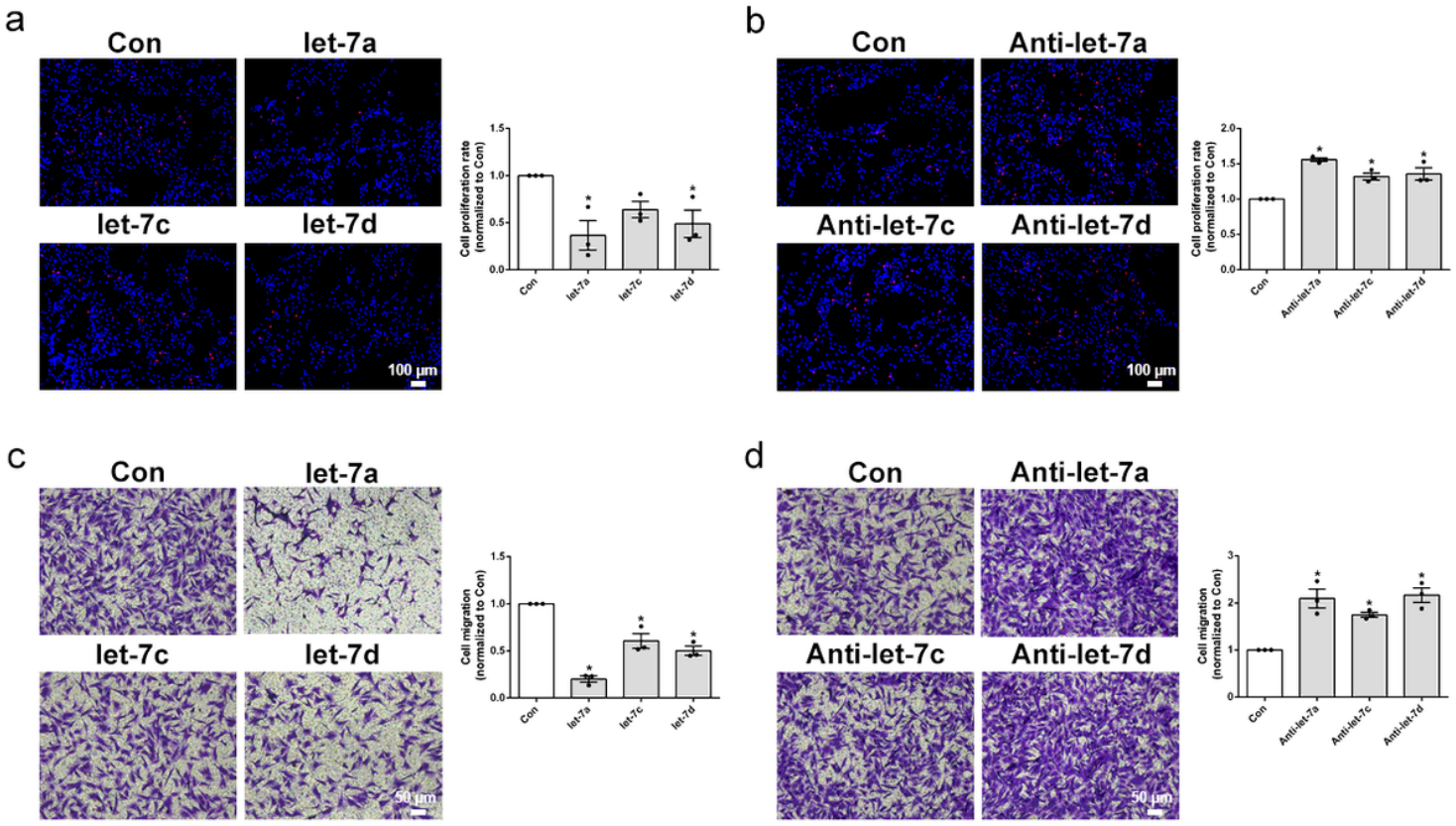

Figure 3

Effect of let-7a, let-7c, and let-7d on Schwann cell proliferation and migration. (a) Merged images of EdU staining (red) and Hoechst 33342 staining (blue) for Schwann cells transfected with let-7a mimic (let-7a), let-7c mimic (let-7c), let-7d mimic (let-7d), and mimic control (Con). (b) Merged images of EdU staining and Hoechst 33342 staining for Schwann cells transfected with let-7a inhibitor (Anti-let-7a), let-7c inhibitor (Anti-let-7c), let-7d inhibitor (Anti-let-7d), and inhibitor control (Con). (c) Images of migrated Schwann cells after transfection with let-7a mimic, let-7c mimic, let-7d mimic, and mimic control. (d) Images of migrated Schwann cells after transfection with let-7a inhibitor, let-7c inhibitor, let-7d inhibitor, and inhibitor control. *p-value < 0.05.

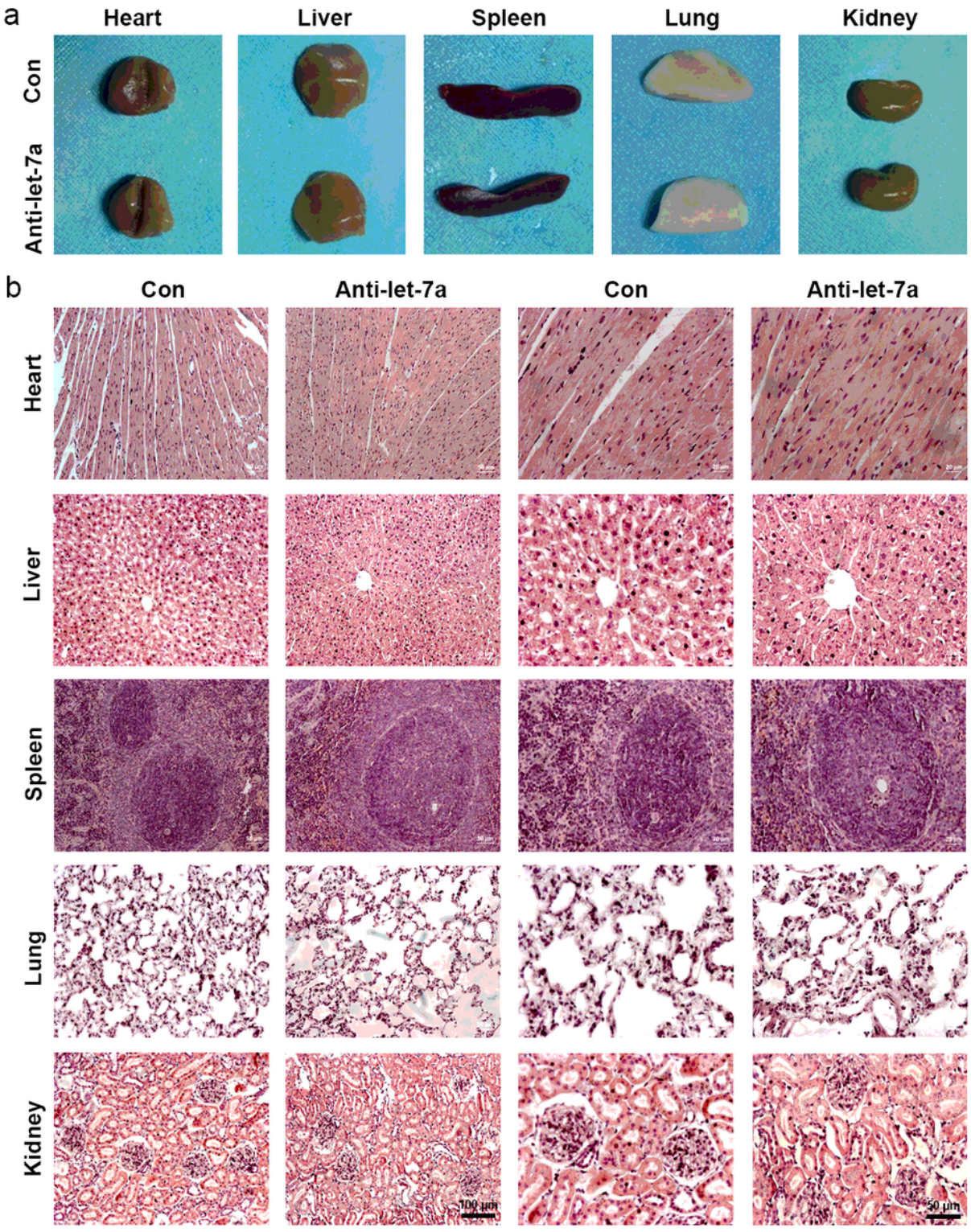

Figure 4

Safety examinations of rats injected with let-7a antagomir. (a) General observation of heart, liver, spleen, lung and kidney in rats injected with saline (Con) or let-7a antagomir (Anti-let-7a) for 5 days. (b) Hetamotylin-eosin staining of heart, liver, spleen, lung, and kidney in rats injected with let-7a antagomir or saline for 5 days. Magnifications were 20 × and 40 ×.

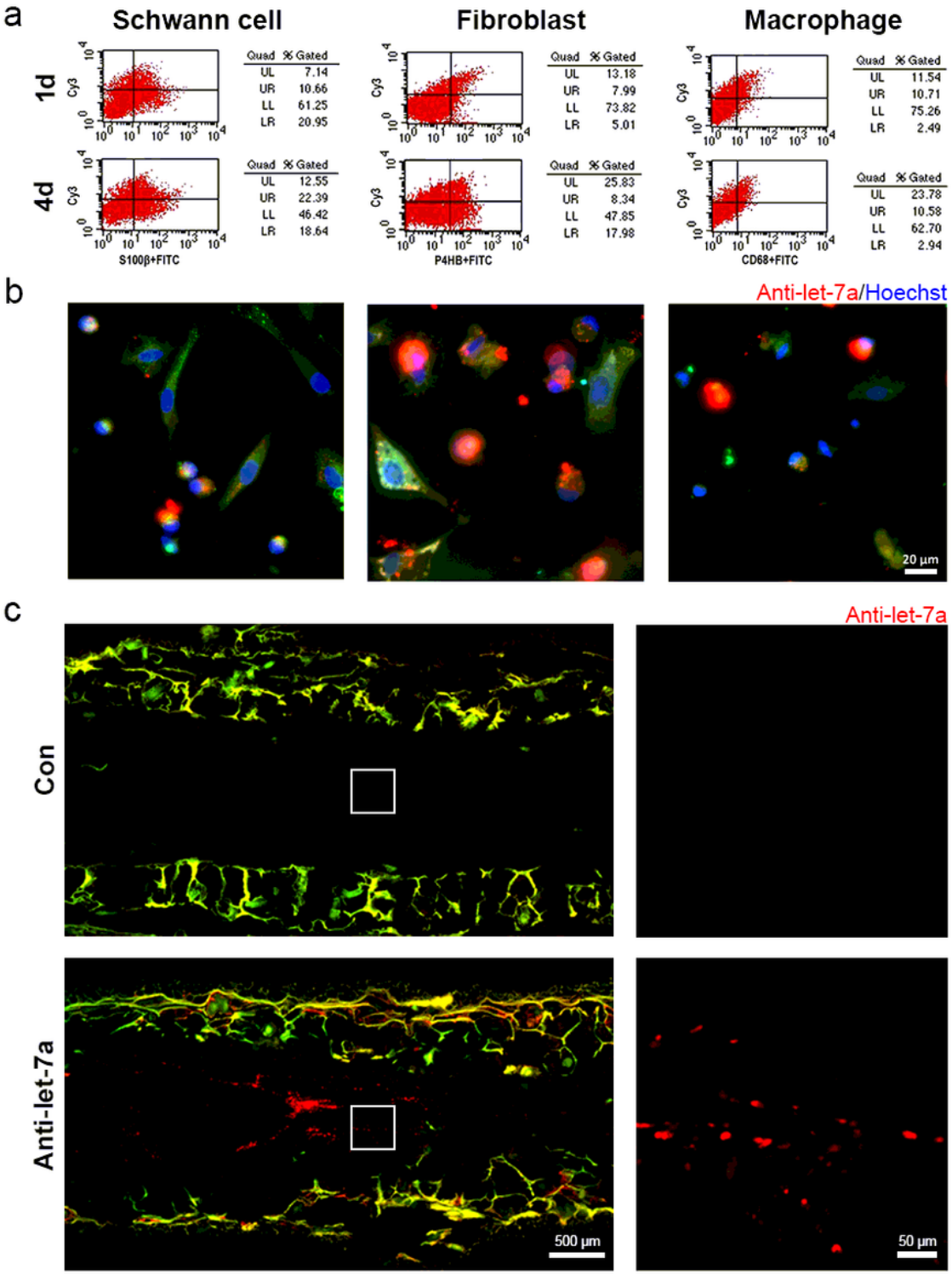

Figure 5

The in vivo localization of let-7a. (a) Flow cytometry of Cy3-labeled let-7a antagomir in Schwann cells, fibroblasts, and macrophages at 1 and 4 days after sciatic nerve injury and let-7a antagomir injection. (b) Merged images of anti-S100β (green), anti-P4HB (green), or anti-CD68 (green) staining, Hoechst 33342 (blue), and Cy3-labeled let-7a antagomir (red) in Schwann cells, fibroblasts, and macrophages (Bar=20 μm) at 4 days after sciatic nerve injury. (c) Fluorescence detection of Cy3-labeled let-7a antagomir at 4

weeks after surgery in nerves bridged with let-7a antagomir (Anti-let-7a) or chitosan-hydrogel scaffold containing non-targeting antagomir control (Con).

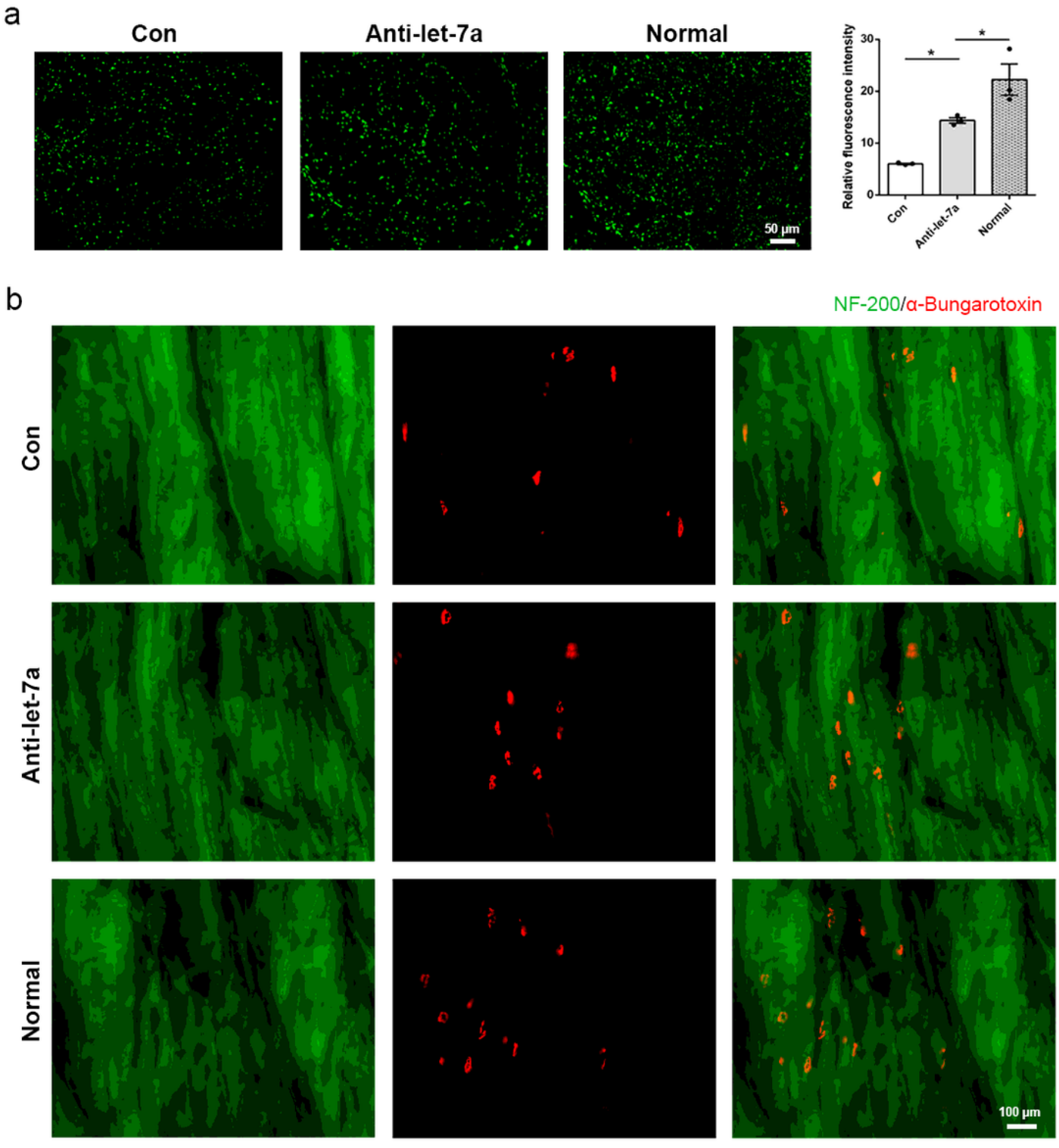

Figure 6

Immunohistochemistry examinations of rat sciatic nerves. (a) NF-200 staining of axons in the transverse sections of normal distal nerve stumps (Normal) and distal nerve stumps bridged with let-7a antagomir (Anti-let-7a) or chitosan-hydrogel scaffold containing non-targeting antagomir control (Con) for 8 weeks.

(b) NF-200 (green) and α-Bungarotoxin (red) staining of the motor endplates at 8 weeks after surgery in transverse sections of gastrocnemius muscles. *p-value < 0.05.

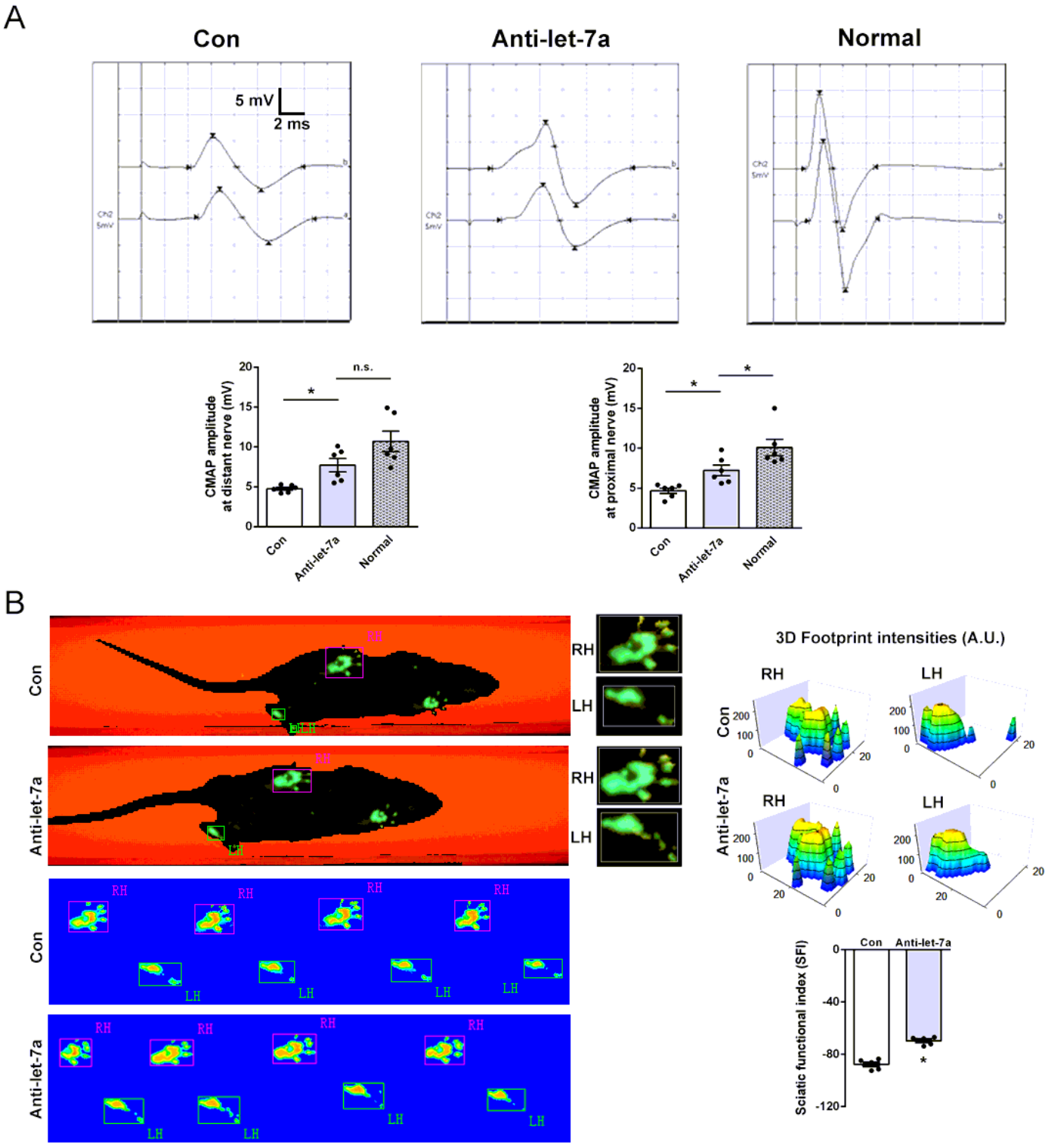

Figure 7

Functional examinations of rat sciatic nerves. (a) CMAP recordings of normal rat sciatic nerves (Normal) and injured nerves bridged with let-7a antagomir (Anti-let-7a) or chitosan-hydrogel scaffold containing non-targeting antagomir control (Con) for 8 weeks. Histogram showed peak CMAP amplitudes at the

proximal and the distal nerve. (b) Representative rat paw print images in CatWalk gait analysis and calculated SCI from CatWalk recordings of the paws of injured rats at 8 weeks after surgery. *p-value < 0.05.

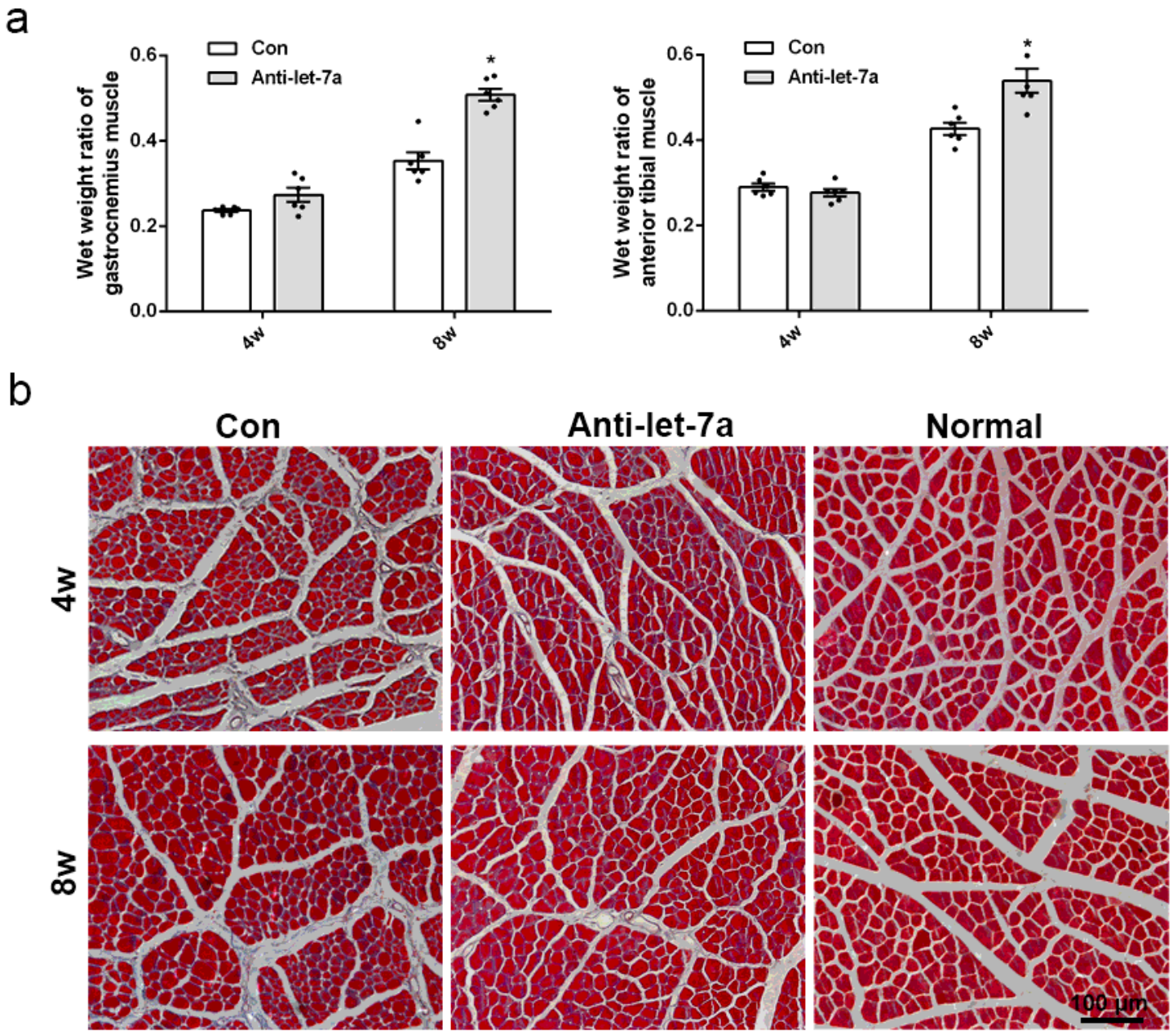

Figure 8

Immunohistochemistry examinations of muscles. (a) Wet weight ratios of gastrocnemius and anterior tibialis muscles of rats bridged with let-7a antagomir (Anti-let-7a) or chitosan-hydrogel scaffold containing non-targeting antagomir control (Con) for 4 and 8 weeks. (b) Masson trichrome staining of gastrocnemius muscle of normal rats (Normal) and nerve injured rats at 4 and 8 weeks after surgery. Red indicated muscle fiber staining and blue indicated collagen fiber staining. *p-value < 0.05.